Polaron effects in asymmetric semiconductor quantum-well structures

Jun-jie Shi
*China Center of Advanced Science and Technology (World Laboratory), P.O. Box 8730, Beijing 100080, China and Department of Physics, Henan Normal University, Xinxiang 453002, Henan, China**

Xiu-qin Zhu† and Zi-xin Liu
Department of Physics, Henan Normal University, Xinxiang 453002, Henan, China

Shao-hua Pan
China Center of Advanced Science and Technology (World Laboratory), P.O. Box 8730, Beijing 100080, China and Institute of Physics, Chinese Academy of Sciences, P.O. Box 603, Beijing 100080, China‡

Xing-yi Li
Department of Physics, Henan Normal University, Xinxiang 453002, Henan, China

(Received 12 March 1996; revised manuscript received 27 August 1996)

In this paper, polaron effects in asymmetric quantum-well structures (QW's) are investigated by using second-order perturbation theory and the modified Lee-Low-Pines (LLP) variational method. By applying the Green's-function method, explicit analytical expressions for the electron extended-state wave functions and the density of states in a general step QW's are given. Within the framework of second-order perturbation theory, the ground-state polaron binding energy and effective mass in step and asymmetric single QW's are studied as due to the interface optical phonons, confined bulklike LO and half-space LO phonons. The full energy spectrum is included in our calculations. The effects of the finite electronic confinement potential and the subband nonparabolicity are also considered. The relative importance of the different phonon modes is analyzed. By means of the modified LLP variational method, the binding energy of a polaron confined to asymmetric single QW's is also investigated. Our results show that in ordinary asymmetric QW's, the asymmetry of the QW's has a significant influence on the polaron effect, which has a close relationship to the interface phonon dispersion. When the well width and one side barrier height of asymmetric single QW's are fixed and identical with those of symmetric QW's, the polaron binding energy in asymmetric QW's is always smaller than that in symmetric QW's. We have also found that it is necessary to include the continuum energy spectrum as intermediate states in the perturbation calculations in order to obtain the correct results; the subband nonparabolicity has a small influence on the polaron effect. Comparing our results obtained by using two different methods, good agreement is found. [S0163-1829(97)03704-1]

I. INTRODUCTION

In recent years, there have been several investigations of polaron effects in polar semiconductor heterostructures such as dielectric slabs, heterojunctions, quantum wires, quantum boxes and quantum-well structures (QW's). It is well known that an electron moving slowly in a heterostructure of polar crystals may cause a distortion of the lattice, establishing a polarization field which acts back on the electron whose properties are then modified; in particular, the electron acquires a self-energy and an enhancement of its Bloch effective mass. The single electron, together with its accompanying distortion, is called a polaron. Some usual QW's, such as $GaAs/Al_xGa_{1-x}As$ QW's, are composed of polar compounds in which the interaction of an electron with optical phonons is an important mechanism that needs to be studied in detail. The polaron effects can strongly influence the optical and transport properties of the heterostructures. Hence the polaron has been a major topic of great interest for a long time.

Polarons in a bulk material have been investigated for many years. Numerous mathematical techniques have been applied to the polaron problem. Excellent reviews have been given by Mitra, Chatterjee, and Mukhopadhyay[1] and Peeters and Devreese.[2] The polaronic effects in polar semiconductor heterostructures are markedly different from those in bulk materials due to the presence of their heterointerfaces. Recently, there has been considerable interest in the electronic properties of the heterostructures of polar crystals. Because the polaron problem in semiconductor heterostructures is much more complicated than that in bulk materials, some approximation methods must be used. The major ones are the perturbation theory, the Lee-Low-Pines (LLP) variational method,[3] the Landau and Pekar variational calculation,[4] and the Green's-function method. Within the framework of second-order perturbation theory, Licari[5] and Liang, Gu, and Lin[6] studied the polaron states in a polar slab. The polaron effects in a heterojunction were investigated by Degani and Hipólito.[7] Lin, Chen, and George,[8] and Hai, Peeters, and Devreese[9] further studied the electron-phonon interaction and the polaron states in a symmetric single QW. A polaron in a symmetric single QW within an electric field has also been investigated by Chen, Liang, and Li.[10] The interface polaron in a heterojunction in a magnetic field was studied by Ban, Liang, and Zheng.[11] Magnetopolarons in a QW have been investigated in the case of a weak external magnetic field in Ref. 12. Haupt and Wendler[13] studied the resonant

magnetopolaron effects in parabolic QW's. Magnetopolarons in quantum dots were investigated in Ref. 14. Hai, Peeters, and Devreese[15] have further studied the magnetopolaron in a GaAs/AlAs symmetric QW. The self-trapping energy of a polaron in a polar-crystal slab in a magnetic field has been obtained by Wei, Zhao, and Gu,[16] who used the Larsen perturbation-theory method. By means of the modified LLP variational method, Ercelebi and Tomak[17] investigated polaron effects in GaAs/$Ga_{1-x}Al_xAs$ QW's, using the infinite-square-well approximation. Surface polarons in a bilayer system are given in Ref. 18. The bound polarons in a heterojunction were studied by Farias, Degani, and Hipólito.[19] The binding energies of bound polarons in strong magnetic fields in a QW, a quantum-well wire, and a quantum box were given in Ref. 20. The properties of a polaron in a polar-crystal slab were also given by Lu and Li.[21] Magnetopolarons in cylindrical quantum wires were investigated by Zhou and Gu.[22] Bound magnetic polarons in a QW were given in Ref. 23. Impurity bound polarons in quantum-well wires were also studied by Zhou and Gu.[24] In the infinite-square-well approximation, Thilagam and Singh[25] investigated polarons in quasi-two-dimensional structures, in which only confined bulklike LO phonons were considered. Furthermore, Zheng, Ban, and Liang[26] considered confined bulklike LO and interface phonons, and studied the properties of a polaron in an infinite QW. Using the Landau-Pekar theory, a strong-coupling theory of quasi-two-dimensional polarons was proposed in Ref. 27, in which the contribution of the interface modes to the polaron effects is ignored. Magnetopolarons in a heterojunction were investigated by means of Green's-function method in Refs. 28 and 29. Knowledge of the behavior of a polaron confined to a finite QW, including all the phonon modes, will be needed for further theoretical investigations and for device applications.

Recently, asymmetric QW's, such as asymmetric single and step QW's, have attracted much attention for some special device applications.[30–36] Optical-phonon modes, electron-phonon interaction, and scattering in asymmetric single and step QW's have been investigated in Refs. 31–36. Some interesting results, such as the frequency-forbidden behavior of the interface optical (IO) modes and the anomalous phenomenon of the electron-phonon interaction in asymmetric QW's have been found. However, to our knowledge, little work has been done about the polaron effects in asymmetric single and step QW's, which are of great theoretical and practical importance at present. Hence it is worthwhile investigating the polaron properties in these asymmetric QW's. The goal of the present paper is to investigate the polaron binding energy and effective mass in asymmetric single and step QW's by means of the second-order perturbation theory and the modified LLP variational method, in which all the possible phonon modes are incorporated and the full electron energy spectrum, i.e., the discrete energy levels in the well and the continuum energy spectrum above the barrier, are all included as intermediate states. The finite barrier height and the conduction band nonparabolicity are also considered.

The present paper is organized as follows. In Sec. II, we outline the theory of polaron binding energy and effective mass. In Sec. III, we present and discuss our numerical results. Section IV gives a summary, which also contains our main conclusions.

II. THEORY

A. Hamiltonian

We consider a general step QW composed of four different polar crystals as shown in Fig. 1 of Ref. 32, which can be regarded as a generalized structure of some important QW's, such as commonly used step QW's and asymmetric and symmetric single QW's. The total Hamiltonian for the coupling of an electron to the optical phonons in this system is described by

$$H=H_e+H_{\mathrm{LO}}+H_{\mathrm{IO}}+H_{e\text{-LO}}+H_{e\text{-IO}}. \tag{1}$$

The first term is the Hamiltonian of an electron confined within a potential well $V(z)$ in the z direction and can be written as

$$H_e=\frac{\mathbf{p}^2}{2m_b}+V(z), \tag{2}$$

with the confinement potential

$$V(z)=\begin{cases} V_l, & z<-a \\ V_w(=0), & -a\leqslant z\leqslant 0 \\ V_s, & 0\leqslant z\leqslant b \\ V_r, & z>b, \end{cases} \tag{3}$$

where $\mathbf{p}$ is electron momentum operator. Considering the subband nonparabolicity, the electron effective mass m_b is given by[37]

$$m_b=\begin{cases} m_l(E)=m_l[1-(V_l-E)/E_{gl}], & z<-a \\ m_w(E)=m_w[1-(V_w-E)/E_{gw}], & -a\leqslant z\leqslant 0 \\ m_s(E)=m_s[1-(V_s-E)/E_{gs}], & 0\leqslant z\leqslant b \\ m_r(E)=m_r[1-(V_r-E)/E_{gr}], & z>b, \end{cases} \tag{4}$$

where $E_{g\nu}$ is the energy gap between the conduction and light-hole valence bands in the material ν ($\nu=l,w,s,r$), and E is the electron energy. m_ν is the electron band mass constant in material ν. The second and third terms in Eq. (1) stand for the LO and IO phonon Hamiltonians, and can be written

$$H_{\mathrm{LO}}=\sum_{\nu,j,\mathbf{k}_\parallel}\hbar\omega_{L\nu}[a^+_{\nu j}(\mathbf{k}_\parallel)a_{\nu j}(\mathbf{k}_\parallel)+\tfrac{1}{2}],$$
$$H_{\mathrm{IO}}=\sum_{m,\mathbf{k}_\parallel}\hbar\omega_m(k_\parallel)[a^+_m(\mathbf{k}_\parallel)a_m(\mathbf{k}_\parallel)+\tfrac{1}{2}], \tag{5}$$

where $\hbar\omega_{L\nu}$ is the bulklike LO-phonon energy in material ν and $\hbar\omega_m(k_\parallel)$ is the IO-phonon energy which can be obtained by solving dispersion relation (12) of Ref. 31. The index m (=1, 2, 3, 4, 5, and 6) labels the six branches of the IO phonons for step QW's, and m (=1, 2, 3, and 4) for asymmetric single QW's.

The fourth term $H_{e\text{-LO}}$ in Eq. (1) is the electron–LO-phonon interaction Fröhlich-like Hamiltonian, and can be written as[33,34]

$$H_{e\text{-LO}}=\sum_{\nu,j,\mathbf{k}_\parallel}e^{i\mathbf{k}_\parallel\cdot\boldsymbol{\rho}}\Gamma^L_{\nu j}(k_\parallel,z)[a_{\nu j}(\mathbf{k}_\parallel)+a^+_{\nu j}(-\mathbf{k}_\parallel)], \tag{6}$$

where $(\boldsymbol{\rho},z)$ is the position vector of the electron, and $\Gamma_{\nu j}^{L}$ is the electron–LO-phonon coupling function, which describes the coupling strength of a single electron with the jth LO mode of layer ν ($\nu=l,w,s,r$) and is given as follows:

$$\Gamma_{\nu j}^{L}(k_{\parallel},z)=\left(\frac{\hbar e^2}{A\varepsilon_0}\right)^{1/2}\left(\frac{\omega_{L\nu}}{T_\nu}\right)^{1/2}\left(\frac{1}{\epsilon_{\infty\nu}}-\frac{1}{\epsilon_{0\nu}}\right)^{1/2}\times\frac{1}{[k_{\parallel}^2+(q_\nu^j)^2]^{1/2}}\,u(q_\nu^j,z),$$

$$u(q_\nu^j,z)\equiv\begin{cases}\sin[q_l^j(z+a)], & -L<z\leqslant a\\ \sin(q_w^j z), & -a\leqslant z<0\\ \sin(q_s^j z), & 0\leqslant z\leqslant b\\ \sin[q_r^j(z-b)], & b\leqslant z<L,\end{cases}\tag{7}$$

$$q_\nu^j=\frac{j\pi}{T_\nu},\quad j=1,2,3,\ldots j_{\max},\quad j_{\max}=\mathrm{int}\left[\frac{T_\nu}{a_{0\nu}}\right],$$

where A is the cross-sectional area of the heterostructure and ε_0 is the absolute dielectric constant. $\epsilon_{0\nu}$ and $\epsilon_{\infty\nu}$ are, respectively, the static and high-frequency dielectric constant. $a_{0\nu}$ is the lattice constant of layer ν, int[x] means the integral part of x, and T_ν is the thickness of layer ν and is given as

$$T_l=L-a,\quad T_w=a,\quad T_s=b,\quad T_r=L-b.\tag{8}$$

Note that for the half-space LO phonons the sum over j in Eq. (6) transforms into an integration, because their momenta in the z direction, i.e., q_l and q_r, become continuous when $L\to\infty$.

The last term in Eq. (1) is the electron–IO-phonon interaction Hamiltonian, which has been given in Sec. II A of Ref. 32.

B. Bare electron states

The bound-electron subband states in our general step QW were given in Sec. II B of Ref. 32, which are localized at the inside of the QW's. In the following, we will only study the electron extended states in the two energy regions $V_l\leqslant E<V_r$ (for definiteness, assuming $V_l\leqslant V_r$) and $E\geqslant V_r$, respectively. We consider the case when the total sample length $2L$ is much larger than the well width; in fact, we will assume that $L\to\infty$.

(1) $V_l\leqslant E<V_r$ case.

In this case, the electron energy spectrum is continuous and nondegenerate.[38] Assuming the usual effective-mass approximation for the conduction band and by using the Bastard boundary condition,[39] the normalized electron extended-state wave function in our general step QW can be obtained from the solution of the Schrödinger equation as follows:

$$\psi(z)=\begin{cases}\left(\frac{2}{L}\right)^{1/2}\cos(k_l z+\alpha), & -L<z\leqslant -a\\ B\cos(k_w z+\beta), & -a\leqslant z<0\\ C\cos(k_s z+\delta), & 0\leqslant z<b\\ De^{-k_r z}, & b\leqslant z<L,\end{cases}\tag{9}$$

where $k_i=\sqrt{2m_i(E)(E-V_i)}/\hbar$ $(i=l,w,s)$ and $k_r=\sqrt{2m_r(E)(V_r-E)}/\hbar$, with E being the electron energy. The constants B, C, D, α, β, and δ in Eq. (9) can be easily determined by the boundary and the normalization conditions.

The density of states $\rho_1(E)$ in the region $V_l\leqslant E<V_r$ can be obtained by using the Green's-function method[40] and by using the infinite boundary condition $G\to 0$ (G the Green's function) as $|z|\to\infty$ and the Bastard boundary condition as follows:

$$\rho_1(E)=\frac{L\sqrt{2m_l}}{\pi\hbar}\frac{1}{\sqrt{E-V_l}}.\tag{10}$$

Here the electron spin corrective factor has been considered.

(2) $E\geqslant V_r(\geqslant V_l)$ case.

In this case, the electron energy spectrum is continuous and twofold degenerate.[38] Hence the electron Hamiltonian has two linearly independent eigenfunctions, which can be obtained from the solutions of the Schrödinger equation as follows:

$$\psi_1(z)=\begin{cases}C_1\cos(k_l z-\xi), & -L<z\leqslant -a\\ C_2\cos(k_w z+\alpha), & -a\leqslant z<0\\ C_3\cos(k_s z+\beta), & 0\leqslant z<b\\ C_4\cos(k_r z+\xi), & b\leqslant z<L,\end{cases}\tag{11a}$$

and

$$\psi_2(z)=\begin{cases}C_1'\sin(k_l z-\xi'), & -L<z\leqslant -a\\ C_2'\sin(k_w z+\alpha'), & -a\leqslant z<0\\ C_3'\sin(k_s z+\beta'), & 0\leqslant z<b\\ C_4'\sin(k_r z+\xi'), & b\leqslant z<L,\end{cases}\tag{11b}$$

where $k_i=\sqrt{2m_i(E)(E-V_i)}/\hbar$ $(i=l,w,s,r)$.

By using an analogous method described in the above, the density of states $\rho_2(E)$ in the region $E\geqslant V_r$ $(\geqslant V_l)$ in our general step QW can be obtained as follows:

$$\rho_2(E)=\frac{\sqrt{2}L}{\pi\hbar}\left[\frac{\sqrt{m_l}}{\sqrt{E-V_l}}+\frac{\sqrt{m_r}}{\sqrt{E-V_r}}\right].\tag{12}$$

Let us now briefly discuss the above results in two cases. When $b=0$, the above results reduce to the corresponding results of an asymmetric single QW. When $b=0$ and $V_l=V_r\equiv V$, the electron extended-state wave functions and the density of states in a symmetric single QW can be obtained from our general results given in the above. In a symmetric single QW case, $\psi_1(z)$ reduces to the symmetric solution $\psi_s(z)$, and $\psi_2(z)$ to the antisymmetric one $\psi_a(z)$ because the structure is symmetric about its center. This conclusion is consistent with the results of Ref. 9 but is not with the results of Ref. 41. The density of states $\rho(E)$ in a symmetric single QW can be immediately obtained from Eq. (12) as

$$\rho(E)=\frac{2\sqrt{2}L}{\pi\hbar}\frac{\sqrt{m}}{\sqrt{E-V}},\tag{13}$$

where $L\to\infty$ and m is the electron effective mass in the barrier layer, and V is the barrier height. Equation (13) is not exactly the same as Eq. (14) of Ref. 42 and the corresponding results of Ref. 9.

By using these results, we obtain the correct polaron binding energy and effective mass (see below). Comparing with the results obtained by the independent variational method (see Sec. II D), which do not use the above electron extended-state wave functions and the density of states, a good agreement is found (see Fig. 2). This indicated in one aspect that the formulas given in this subsection are correct.

C. Polaron energy and effective mass

In this subsection, we will calculate the polaron correction to the ground-state energy and its effective mass in a general step QW. Most of the present-day QW's are made out of weak polar semiconductors, and consequently we are allowed to use second-order perturbation theory. Based on this theory, the energy of a polaron in the ground state is given by

$$E = E_{\parallel} + E_1^z - \Delta E, \tag{14}$$

where $E_{\parallel} = \mathbf{p}_{\parallel}^2/2m_{\parallel}$ is the energy, $\mathbf{p}_{\parallel}$ being the electron momentum and $m_{\parallel}$ the effective mass in the xy plane, respectively. E_1^z is the ground-state energy for the electron motion in the z direction. ΔE is the binding energy of a polaron due to the different phonon modes at the bottom of the first level and is given by

$$\Delta E = \Delta E^{(1)} + \Delta E^{(2)} + \Delta E^{(3)}, \tag{15}$$

where

$$\Delta E^{(1)} = \frac{A}{2\pi} \sum_{n=1}^{n_{\max}} f_1(E_n^z),$$

$$\Delta E^{(2)} = \frac{A}{2\pi} \int_{V_l}^{V_r} \rho_1(E) f_1(E) dE, \tag{16}$$

$$\Delta E^{(3)} = \frac{A}{2\pi} \int_{V_r}^{\infty} \rho_2(E) f_1(E) dE.$$

In Eq. (16), $n_{\max}$ is the number of the discrete energy levels in our general step QW, and the definition of function $f_1(E)$ is given by

$$\begin{aligned} f_1(E) = & \sum_{m=1}^{6} \int_0^{\infty} dk_{\parallel} \frac{k_{\parallel} |M_{1,n}^m(k_{\parallel})|^2}{\hbar\omega_m(k_{\parallel}) + E - E_1^z + \hbar^2 k_{\parallel}^2/2m_{\parallel}} \\ & + \sum_{\mu=w,s} \sum_{j=1}^{j_{\max}} \int_0^{\infty} dk_{\parallel} \frac{k_{\parallel} |M_{1,n}^{\mu j}(k_{\parallel})|^2}{\hbar\omega_{L\mu} + E - E_1^z + \hbar^2 k_{\parallel}^2/2m_{\parallel}} \\ & + \sum_{\nu=l,r} \int_0^{\infty} dq_{\nu} \int_0^{\infty} dk_{\parallel} \frac{k_{\parallel} |M_{1,n}^{\nu j}(k_{\parallel})|^2}{\hbar\omega_{L\nu} + E - E_1^z + \hbar^2 k_{\parallel}^2/2m_{\parallel}}. \end{aligned} \tag{17}$$

The corresponding polaron effective mass can be obtained from the formula

$$\frac{1}{m^*} \equiv \frac{1}{\hbar^2} \frac{d^2E}{dk^2}$$

as follows:

$$m^* \doteq m_{\parallel} + \Delta m, \tag{18}$$

where Δm is the effective-mass correction due to the electron-phonon interaction, and is given by

$$\Delta m = \Delta m^{(1)} + \Delta m^{(2)} + \Delta m^{(3)}, \tag{19}$$

with

$$\Delta m^{(1)} = \frac{A}{2\pi} \sum_{n=1}^{n_{\max}} f_2(E_n^z),$$

$$\Delta m^{(2)} = \frac{A}{2\pi} \int_{V_l}^{V_r} \rho_1(E) f_2(E) dE, \tag{20}$$

$$\Delta m^{(3)} = \frac{A}{2\pi} \int_{V_r}^{\infty} \rho_2(E) f_2(E) dE,$$

where the function $f_2(E)$ is defined as

$$\begin{aligned} f_2(E) = & \sum_{m=1}^{6} \int_0^{\infty} dk_{\parallel} \frac{\hbar^2 k_{\parallel}^3 |M_{1,n}^m(k_{\parallel})|^2}{[\hbar\omega_m(k_{\parallel}) + E - E_1^z + \hbar^2 k_{\parallel}^2/2m_{\parallel}]^3} \\ & + \sum_{\mu=w,s} \sum_{j=1}^{j_{\max}} \int_0^{\infty} dk_{\parallel} \frac{\hbar^2 k_{\parallel}^3 |M_{1,n}^{\mu j}(k_{\parallel})|^2}{[\hbar\omega_{L\mu} + E - E_1^z + \hbar^2 k_{\parallel}^2/2m_{\parallel}]^3} \\ & + \sum_{\nu=l,r} \int_0^{\infty} dq_{\nu} \\ & \times \int_0^{\infty} dk_{\parallel} \frac{\hbar^2 k_{\parallel}^3 |M_{1,n}^{\nu j}(k_{\parallel})|^2}{[\hbar\omega_{L\nu} + E - E_1^z + \hbar^2 k_{\parallel}^2/2m_{\parallel}]^3}. \end{aligned} \tag{21}$$

In Eqs. (17) and (21), $M_{1,n}^{m}(k_{\parallel})$, $M_{1,n}^{\mu j}(k_{\parallel})$, and $M_{1,n}^{\nu j}(k_{\parallel})$ are the electron-IO, electron confined-LO, and electron–half-space–LO-phonon interaction matrix elements, respectively.

D. Variational calculation of the polaron energy

For the sake of comparison, in this subsection we will further investigate the polaron binding energy by using the modified LLP variational method in asymmetric single QW's ($b=0$) for simplicity, which has no direct connection with the perturbation method. The following formulas can be easily extended to the step QW. Consider the following ansatz to the polaron wave function:

$$|\psi\rangle = U\phi_n(z)|0\rangle, \tag{22}$$

where $\phi_n(z)$ is the electron wave function in the z direction, and is given as

$$\phi_n(z) = \begin{cases} \phi_{ln} = B_n A_{ln} e^{k_{ln} z}, & z < 0 \\ \phi_{wn} = B_n [A_{wn} \sin(k_{wn} z) + A_{ln} \cos(k_{wn} z)], & 0 \leq z \leq a \\ \phi_{rn} = B_n e^{-k_{rn} z}, & z > a, \end{cases} \tag{23}$$

where $k_{\nu n} \equiv [2m_{\nu}(E_n^{(0)})(V_{\nu} - E_n^{(0)})]^{1/2}/\hbar$ $(\nu = l,r)$ and $k_{wn} \equiv [2m_w(E_n^{(0)})E_n^{(0)}]^{1/2}/\hbar$, with $E_n^{(0)}$ being the nth eigenvalue of the electron Hamiltonian H_e and can be determined by the following Eq. (25). A_{ln}, A_{wn}, and B_n are defined as

$$A_{ln}=e^{-k_{rn}a}/[f_{wln}\sin(k_{wn}a)+\cos(k_{wn}a)],$$

$$A_{wn}=A_{ln}f_{wln}, \tag{24}$$

$$B_n=e^{k_{rn}a}\left\{\frac{1}{2k_{rn}}+[f_{wln}\sin(k_{wn}a)+\cos(k_{wn}a)]^{-2}\times\left[\frac{1}{2k_{ln}}+\frac{a}{2}+\frac{\sin(2k_{wn}a)}{4k_{wn}}+f_{wln}^2\left(\frac{a}{2}-\frac{\sin(2k_{wn}a)}{4k_{wn}}\right)+f_{wln}\frac{\sin^2(k_{wn}a)}{k_{wn}}\right]\right\}^{-1/2}.$$

The subband energy equation in our asymmetric single QW potential is obtained as

$$(f_{wrn}f_{wln}-1)\sin(k_{wn}a)+(f_{wrn}+f_{wln})\cos(k_{wn}a)=0, \tag{25}$$

where

$$f_{wrn}\equiv\frac{m_w(E)k_{rn}}{k_{wn}m_r(E)},\quad f_{wln}\equiv\frac{m_w(E)k_{ln}}{k_{wn}m_l(E)}. \tag{26}$$

In Eq. (22), $|0\rangle$ is the phonon vacuum state, and the canonical transformation U is given by

$$U=U_1U_2,$$

$$U_1=\exp\left\{\sum_{\nu,j,\mathbf{k}_\parallel}[\gamma_{\nu j\mathbf{k}_\parallel}(\boldsymbol{\rho},z)a^+_{\nu j\mathbf{k}_\parallel}-\gamma^*_{\nu j\mathbf{k}_\parallel}(\boldsymbol{\rho},z)a_{\nu j\mathbf{k}_\parallel}]\right\}, \tag{27}$$

$$U_2=\exp\left\{\sum_{i,\mathbf{k}_\parallel}[\gamma_{i\mathbf{k}_\parallel}(\boldsymbol{\rho})a^+_{i\mathbf{k}_\parallel}-\gamma^*_{i\mathbf{k}_\parallel}(\boldsymbol{\rho})a_{i\mathbf{k}_\parallel}]\right\},$$

where

$$\gamma_{\nu j\mathbf{k}_\parallel}(\boldsymbol{\rho},z)=\alpha_{\nu j\mathbf{k}_\parallel}u(q^j_\nu,z)e^{-i\mathbf{k}_\parallel\cdot\boldsymbol{\rho}},$$

$$\gamma_{i\mathbf{k}_\parallel}(\boldsymbol{\rho})=\beta_{i\mathbf{k}_\parallel}e^{-i\mathbf{k}_\parallel\cdot\boldsymbol{\rho}}, \tag{28}$$

with $\alpha_{\nu j\mathbf{k}_\parallel}$ and $\beta_{i\mathbf{k}_\parallel}$ being the two variational parameters which will subsequently be determined by minimizing the energy of the system. Since we are interested only in the ground state of the polaron, assuming that the momentum of the electron in the xy plane is zero, for simplicity we shall neglect the interaction between the virtual phonons emitted and reabsorbed by the recoiled electron, which is generally very small in the case of weak coupling.[3] The total polaron ground-state energy is obtained by computing the expectation value $\langle\psi|H|\psi\rangle$, which gives

$$E_1=\langle\psi|H|\psi\rangle=E_1^{(0)}+E_1^{(\mathrm{LO})}+E_1^{(\mathrm{IO})}, \tag{29}$$

where $E_1^{(0)}$ is the lowest-energy solution of Eq. (25). $E_1^{(\mathrm{LO})}$ and $E_1^{(\mathrm{IO})}$ are, respectively, the contributions of the electron LO and IO interactions. After lengthy algebra, we can finally obtain explicit analytical expressions of $E_1^{(\mathrm{LO})}$ and $E_1^{(\mathrm{IO})}$ as follows:

$$-E_1^{(\mathrm{LO})}=\sum_{\nu=l,r}\frac{\sigma_\nu}{4\pi}\frac{B_1^2C_\nu}{k_{\nu1}\left[\hbar\omega_{L\nu}+\frac{\hbar^2}{m_\nu}(k_{\nu1})^2\right]}\int_0^\infty dq\,\frac{q^2}{(k_{\nu1})^2+q^2}\ln\left[2\left(\frac{m_\nu\omega_{L\nu}}{\hbar}+(k_{\nu1})^2\right)\frac{1}{q^2}+1\right]$$

$$+\frac{\sigma_w}{a}\sum_{j=1}^{\mathrm{int}[a/a_{02}]}\frac{|\Xi_{wj1}|^2}{\left(\frac{\hbar^2}{2m_w}\frac{j^2\pi^2}{a^2}-\hbar\omega_{Lw}\right)\Xi_{wj1}-\frac{\hbar^2}{2m_w}\frac{j^2\pi^2}{a^2}\Omega_{wj1}}\ln\left[\frac{\frac{\hbar^2}{2m_w}\frac{j^2\pi^2}{a^2}\Xi_{wj1}}{\hbar\omega_{Lw}\Xi_{wj1}+\frac{\hbar^2}{2m_w}\frac{j^2\pi^2}{a^2}\Omega_{wj1}}\right], \tag{30}$$

where

$$\Xi_{wj1}=\frac{B_1^2}{4}\left\{(A_{w1}^2-A_{l1}^2)\left[a-\frac{\sin(2q_w^ja)}{2q_w^j}-\frac{\sin(2k_{w1}a)}{2k_{w1}}+\frac{\sin[2(q_w^j-k_{w1})a]}{4(q_w^j-k_{w1})}+\frac{\sin[2(q_w^j+k_{w1})a]}{4(q_w^j+k_{w1})}\right]+A_{l1}^2\left[2a-\frac{\sin(2q_w^ja)}{q_w^j}\right]\right.$$
$$\left.+A_{w1}A_{l1}\left[\frac{1-\cos(2k_{w1}a)}{k_{w1}}+\frac{\cos[2(k_{w1}+q_w^j)a]-1}{2(k_{w1}+q_w^j)}+\frac{\cos[2(k_{w1}-q_w^j)a]-1}{2(k_{w1}-q_w^j)}\right]\right\},$$

$$\Omega_{wj1}=\frac{B_1^2}{2}\left\{(A_{w1}^2+A_{l1}^2)a+(A_{l1}^2-A_{w1}^2)\frac{\sin(2k_{w1}a)}{2k_{w1}}+\frac{1}{k_{w1}}[1-\cos(2k_{w1}a)]A_{w1}A_{l1}\right\}-\Xi_{wj1}, \tag{31}$$

$$\sigma_\nu=\frac{(\hbar\omega_{L\nu})e^2}{4\pi\varepsilon_0}\left(\frac{1}{\epsilon_{\infty\nu}}-\frac{1}{\epsilon_{0\nu}}\right),\quad \nu=l,w,r,$$

$$C_\nu=\begin{cases}A_{l1}^2, & \nu=l\\ e^{-2k_{r1}a}, & \nu=r\end{cases}$$

and

$$-E_1^{(\mathrm{IO})}=\sum_{i=1}^{4}\frac{\hbar^2e^2}{16\pi\varepsilon_0}\int_0^\infty dk_\parallel\frac{\Lambda_1^2}{\hbar\omega_{ik_\parallel}\Lambda_2\left(\hbar\omega_{ik_\parallel}+\frac{\hbar^2k_\parallel^2}{2\overline{m}_\parallel}\right)},\tag{32}$$

where

$$\begin{aligned}\Lambda_1=B_1^2\Bigg\{&\frac{A_{l1}^2}{2k_{l1}+k_\parallel}(1-r_l)(1-r_w^2)e^{-k_\parallel a}+\frac{e^{-2k_{r1}a}}{2k_{r1}+k_\parallel}(1-r_w)[(1-r_lr_w)+(r_w-r_l)e^{-2k_\parallel a}]\\&+(1-r_w)(r_w-r_l)e^{-k_\parallel a}\Bigg[(A_{w1}^2-A_{l1}^2)\left(f_3(k_\parallel)-\frac{k_\parallel+[2k_{w1}\sin(2k_{w1}a)-k_\parallel\cos(2k_{w1}a)]e^{-k_\parallel a}}{2[(k_\parallel)^2+4(k_{w1})^2]}\right)+2A_{l1}^2f_3(k_\parallel)\\&+A_{w1}A_{l1}\frac{2k_{w1}-e^{-k_\parallel a}[k_\parallel\sin(2k_{w1}a)+2k_{w1}\cos(2k_{w1}a)]}{(k_\parallel)^2+4(k_{w1})^2}\Bigg]+(1-r_w)(1-r_lr_w)\\&\times\Bigg[(A_{w1}^2-A_{l1}^2)\left(f_3(k_\parallel)+\frac{k_\parallel e^{-k_\parallel a}-[2k_{w1}\sin(2k_{w1}a)+k_\parallel\cos(2k_{w1}a)]}{2[(k_\parallel)^2+4(k_{w1})^2]}\right)+2A_{l1}^2f_3(k_\parallel)\\&+A_{w1}A_{l1}\frac{2k_{w1}e^{-k_\parallel a}+[k_\parallel\sin(2k_{w1}a)-2k_{w1}\cos(2k_{w1}a)]}{(k_\parallel)^2+4(k_{w1})^2}\Bigg]\Bigg\},\end{aligned}$$

$$\Lambda_2=D_l(1-r_w^2)^2e^{-2k_\parallel a}+D_w[(1-r_lr_w)^2+(r_l-r_w)^2e^{-2k_\parallel a}](1-e^{-2k_\parallel a})+D_r[(r_l-r_w)e^{-2k_\parallel a}+r_w(1-r_lr_w)]^2,$$

$$f_3(k_\parallel)=\frac{1-e^{-k_\parallel a}}{2k_\parallel},\tag{33}$$

$$D_\nu=\frac{\epsilon_{\infty\nu}^2(\omega_{L\nu}^2-\omega_{T\nu}^2)^2}{\omega_{T\nu}^2(\epsilon_{0\nu}-\epsilon_{\infty\nu})[\epsilon_{\infty\nu}(\omega_{L\nu}^2-\omega_{ik_\parallel}^2)-(\omega_{T\nu}^2-\omega_{ik_\parallel}^2)]^2},$$

$$r_\nu=\frac{\epsilon_\nu(\omega)+1}{\epsilon_\nu(\omega)-1},$$

where $\epsilon_\nu(\omega)$ is the dielectric function of layer ν. Supposing $m_\parallel=m_z$, $1/\overline{m}_\parallel$ in Eq. (32) can be given as

$$\frac{1}{\overline{m}_\parallel}=B_1^2\left\{\frac{A_{l1}^2}{2k_{l1}m_l(E)}+\frac{e^{-2k_{r1}a}}{2k_{r1}m_r(E)}+\frac{1}{m_w(E)}\left[A_{w1}^2\left(\frac{a}{2}-\frac{\sin(2k_{w1}a)}{4k_{w1}}\right)-A_{w1}A_{l1}\frac{\cos(2k_{w1}a)^{-1}}{2k_{w1}}+A_{l1}^2\left(\frac{a}{2}+\frac{\sin(2k_{w1}a)}{4k_{w1}}\right)\right]\right\}.\tag{34}$$

The polaron binding energy ΔE can be defined as

$$\Delta E=E_1^{(0)}-E_1=-E_1^{(\mathrm{LO})}-E_1^{(\mathrm{IO})}.\tag{35}$$

III. NUMERICAL RESULTS AND DISCUSSION

As an application of our theory given in Sec. II, we have performed numerical calculations for the ground-state polaron binding energy and effective mass in GaAs/$Al_xGa_{1-x}As$ asymmetric single and step QW's. The physical parameters used in our calculations are the same as those of Ref. 32. In addition, we take the parameter $E_{g\nu}=1424+1266x_\nu+260x_\nu^2$ meV ($\nu=l,w,s,r$) and the lattice constant[43] $a_{0\nu}=5.6533+0.0078x_\nu$ Å. For convenience, we take $m_\parallel=0.0665m_0$, with m_0 being the free-electron mass.

The polaron binding energy ΔE has been numerically calculated as a function of well width a for $Al_{0.18}Ga_{0.82}As$/GaAs/$Al_{0.42}Ga_{0.58}As$ asymmetric single QW's. We know from our numerical calculations that ΔE is a sensitive function of the interface phonon dispersion. The polaron binding energy may have a remarkable change when the frequency of the interface phonons has a small deviation. The contributions of different phonon modes from the discrete energy levels and the continuum energy spectrum are shown in Figs. 1(a) and 1(b), respectively. We can see the following from Fig. 1. (1) For the half-space LO-phonon modes in the two barrier layers, the contribution from the continuous spectrum plays an important role in narrow QW; for instance, it approaches approximately 85% of the total half-space LO modes contribution at $a=16$ Å. (2) For the confined bulklike LO modes in the well layer, the contribution of them to the polaron binding energy from the continuous spectrum is within about 30% of their total contribution at $a\doteq75$ Å, and 15% at $a\doteq200$ Å. The contributions from the discrete energy

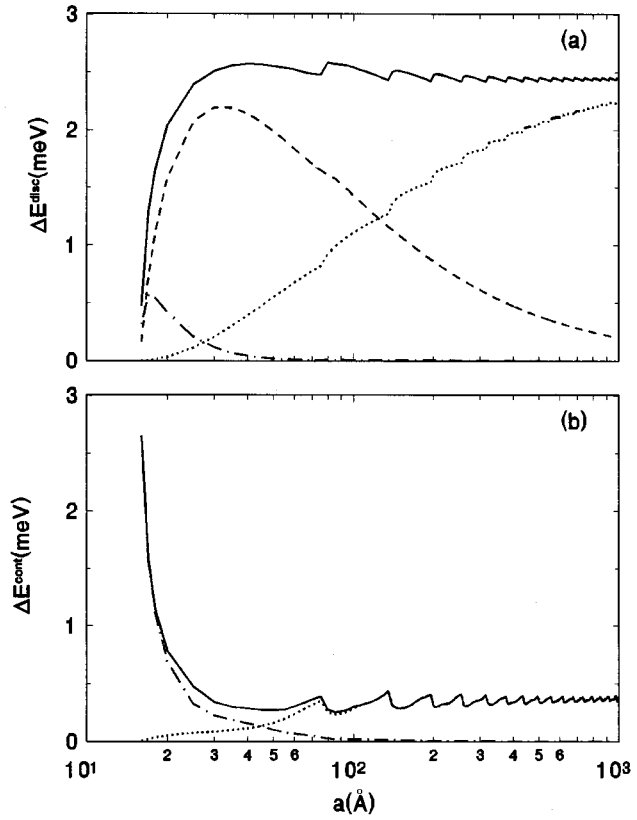

FIG. 1. The contribution of the confined bulklike LO-phonon mode (heavy dotted line), the IO-phonon mode (short-dashed line), and half-space LO-phonon mode (dot-dashed line) to the polaron binding energy from (a) the discrete energy levels in the well and (b) the continuum energy spectrum above the barrier for $Al_{0.18}Ga_{0.82}As/GaAs/Al_{0.42}Ga_{0.58}As$ asymmetric single QW's. Here the solid line gives their summation.

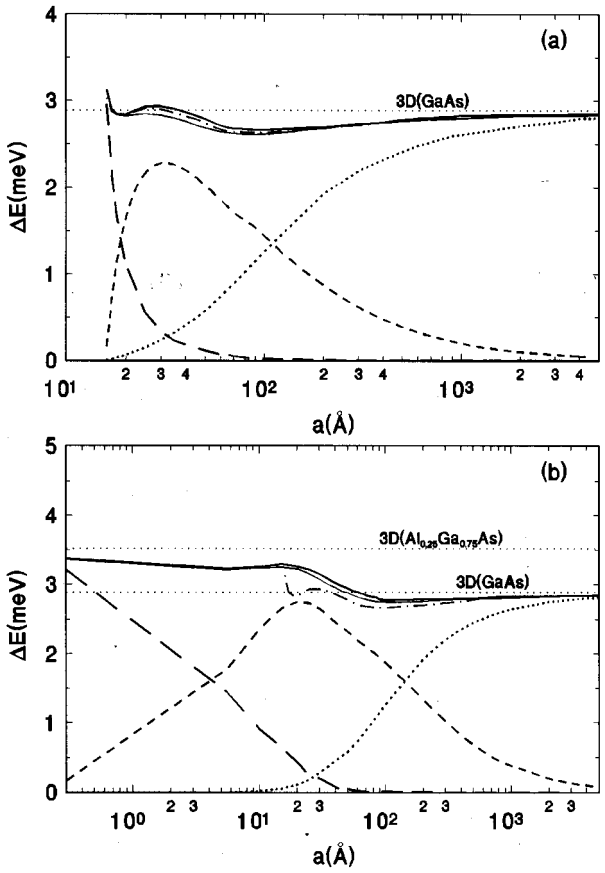

FIG. 2. Polaron binding energy as a function of the well width a for (a) $Al_{0.18}Ga_{0.82}As/GaAs/Al_{0.42}Ga_{0.58}As$ asymmetric and (b) $Al_{0.25}Ga_{0.75}As/GaAs/Al_{0.25}Ga_{0.75}As$ symmetric single QW's. The heavy solid, short-dashed, heavy dotted, and long-dashed lines indicate the total polaron binding energy, the contribution of the IO-, confined bulklike LO-, and the half-space LO-phonon modes, respectively. The dot-dashed line in (a) gives the polaron binding energy in asymmetric QW's, ignoring the subband nonparabolicity. The thin solid line in (a) and (b) shows the polaron binding energy obtained by using LLP variational method. The dot-dashed line in (b) stands for the polaron binding energy in the same structure as in (a).

levels and the continuous spectrum have all a discontinuous derivative each time an energy level enters the quantum well when the well width increases. (3) The contribution of the IO modes comes mainly from the discrete levels, and the contribution of them from the continuous energy spectrum is very small, and has been neglected in Fig. 1(b). As stated in the above, for half-space LO modes in the two barrier layers, the contributions of them to the polaron binding energy come mainly from the continuous spectrum. However, for the confined bulklike LO and IO modes, the contributions from the continuous spectrum is smaller than the corresponding contribution from the discrete energy levels. The contribution of various phonon modes from the continuous spectrum to the polaron energy approaches approximately 80% of the total polaron energy at $a=16$ Å, and 15% for $a>30$ Å. The above results clearly show that it is necessary to include the full energy spectrum and all the possible phonon modes in the study of the polaron effects in a QW. We also calculated the corresponding results for the polaron effective mass, and the results show that the behavior of the polaron effective mass correction due to various phonon modes is similar to that of the binding energy.

The ground-state polaron binding energy as a function of the well width a for $Al_{0.18}Ga_{0.82}As/GaAs/Al_{0.42}Ga_{0.58}As$ asymmetric single QW's is given in Fig. 2(a). The figure clearly shows that in the case when the well width is small, the contribution of the half-space LO modes in the two barrier layers is very important; the polaron binding energy comes mainly from the contribution of the IO modes when the well width 18 Å$<a<$120 Å; the contribution of the confined bulklike LO phonons in GaAs layer is significant in the case of the well width $a>120$ Å. We can also see from Fig. 2(a) that the total polaron binding energy is a complicated function of well width a in the case of $a<100$ Å, and then monotonically increases slowly to the three-dimensional (3D) bulk value of GaAs as the well width is very large. Comparing with our variational calculation results, a good agreement is found. This proves in one aspect that our results for the electron extended states and the density of states in Sec. II B are correct. Figure 2(a) also indicates that the subband nonparabolicity has a small influence on the polaron binding energy. For comparison, the results for $Al_{0.25}Ga_{0.75}As/GaAs/Al_{0.25}Ga_{0.7}As$ symmetric single QW's are also given in Fig. 2(b). The figure shows that the total polaron binding energy ΔE depends very little on the well

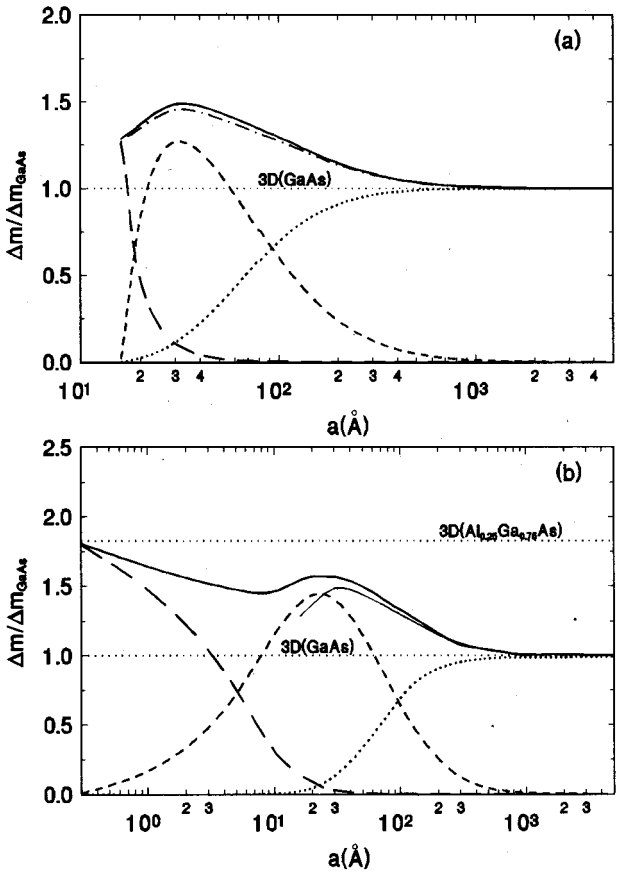

FIG. 3. Same as in Fig. 2, but for the polaron effective mass.

width a in symmetric QW's. Furthermore, in the limiting case $a\rightarrow 0$, the 3D $Al_{0.25}Ga_{0.75}As$ bulk value can be approximately obtained and when the well width $a\rightarrow\infty$, the 3D GaAs bulk value can also be exactly obtained. This is also in agreement with the sum rule established by some authors.[44–46] Comparing Figs. 2(a) and 2(b), we can see that, in the case of asymmetric single QW's, the asymmetry of the structure and the condition that a confined electron state can exist result in a difference of polaron binding energy between asymmetric and symmetric QW's. The smaller the well width, the larger the difference of a polaron binding energy between our symmetric and asymmetric QW's. However, when the well width is very large, the difference between asymmetric and symmetric QW's can be neglected.

The calculation results for the polaron effective mass in $Al_{0.18}Ga_{0.82}As/GaAs/Al_{0.42}Ga_{0.58}As$ asymmetric and $Al_{0.25}Ga_{0.75}As/GaAs/Al_{0.25}Ga_{0.75}As$ symmetric single QW's are shown in Figs. 3(a) and 3(b), respectively, in which we denote the polaron effective-mass correction with respect to the 3D GaAs value $\Delta m_{\mathrm{GaAs}}=\alpha m_w/6$, where α is the electron-phonon Fröhlich coupling constant of GaAs material. The figures show that the situation of the contributions of different phonon modes to the polaron effective mass is similar to that of the contributions to the polaron binding energy shown in Fig. 2. Figure 3(a) also clearly shows that the subband nonparabolicity has a small influence on the polaron effective mass. Comparing Figs. 3(a) and 3(b), we can see that the polaron effective-mass correction in our asymmetric QW's is smaller than that in symmetric QW's in the case $a<300$ Å, and the difference between the two structures can be neglected when the well width $a>300$ Å.

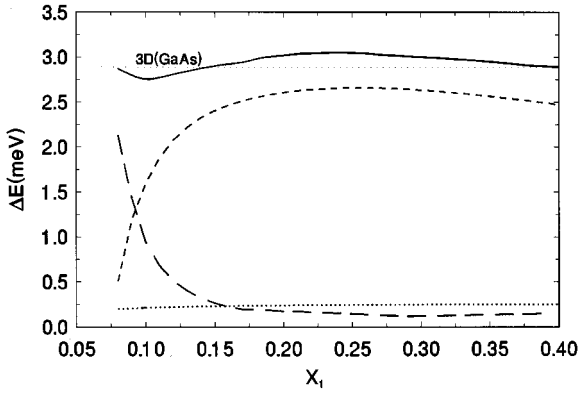

FIG. 4. Polaron binding energy as a function of Al composition x_1 for $Al_{x_1}Ga_{1-x_1}As/GaAs/Al_{0.25}Ga_{0.75}As$ QW's in fixing well width $a=30$ Å. The various lines have the same meaning as in Fig. 2, respectively.

To further investigate the relation between the polaron effect and the asymmetry degree in asymmetric QW's, in Fig. 4 we give the polaron binding energy as a function of Al fraction x_1 (which determines the left barrier height) for $Al_{x_1}Ga_{1-x_1}As/GaAs/Al_{0.25}Ga_{0.75}As$ QW's with fixed well width $a=30$ Å. An interesting result is seen in Fig. 4: the total polaron binding energy in the case $x_1\doteq 0.25$ (symmetric QW) is larger than that in asymmetric QW's. The larger the asymmetry degree $|0.25-x_1|$, the larger the difference of a polaron binding energy between our symmetric and asymmetric QW's. The polaron effective mass as a function of x_1 for a similar structure as in Fig. 4 is also calculated. The results show that the behavior of the polaron effective mass is analogous to that of the binding energy. This indicate that the influence of the asymmetry of the structure on the polaron effect is significant for narrow QW's, which results from the sensitivity of phonon modes and electron wave function on the structure parameters.

Figure 5 shows the polaron binding energy as a function of the well width a for $Al_{0.35}Ga_{0.65}As/GaAs/Al_{0.2}Ga_{0.8}As/Al_{0.4}Ga_{0.6}As$ step QW's with a fixed step width $b=50$ Å. We can see from Fig. 5 that the contributions of the LO phonons in the $Al_{0.2}Ga_{0.8}As$ layer to the polaron binding energy is small, and can be neglected when the well width $a>100$ Å. The contribution of the half-space LO phonons in the two-barrier layers is very small, and can also be neglected when $a>100$ Å. The contribution of the IO phonons and the confined LO phonons in the GaAs layer are important, and similar to those shown in Fig. 2 for asymmetric single QW's. The total polaron binding energy is a complicated function of the well width a and, in the limit $a\rightarrow\infty$, the 3D GaAs bulk value can be exactly obtained. For comparison, we have also calculated the polaron binding energy for $Al_{0.35}Ga_{0.65}As/GaAs/Al_{0.2}Ga_{0.8}As/Al_{0.35}Ga_{0.65}As$ commonly used step QW's. We find that for narrow QW's ($a<200$ Å), the total polaron binding energy in the commonly used step QW's is slightly larger than that in general step QW's, and, when $a>200$ Å, the difference of a polaron binding energy between commonly used and general step QW's can be neglected. Furthermore, the subband nonparabolicity has a small influence on the polaron energy in step QW's.

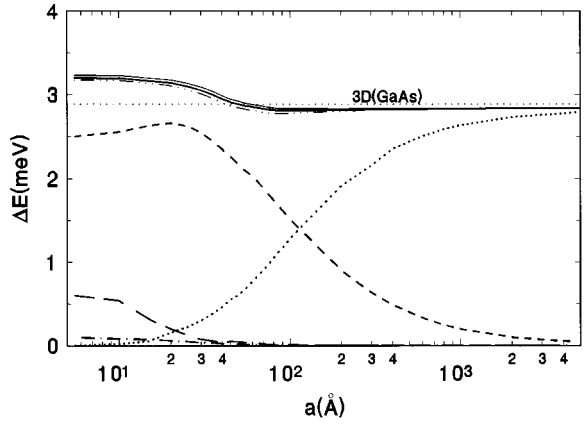

FIG. 5. Polaron binding energy as a function of the well width a for $Al_{0.35}Ga_{0.65}As/GaAs/Al_{0.2}Ga_{0.8}As/Al_{0.4}Ga_{0.6}As$ step QW's in fixing step width $b=50$ Å for the IO modes (the short-dashed line), the half-space LO modes (the dot-dashed line), the confined bulklike LO phonons in the GaAs layer (the heavy dotted line) and those in the $Al_{0.2}Ga_{0.8}As$ layer (the long-dashed line), and their summation (the heavy solid line). Here the dot-dot-dashed line represents the polaron binding energy, ignoring the subband nonparabolicity. The thin solid line indicates the polaron binding energy in commonly used step QW's $Al_{0.35}Ga_{0.65}As/GaAs/Al_{0.2}Ga_{0.8}As/Al_{0.35}Ga_{0.65}As$ with fixing the step width $b=50$ Å.

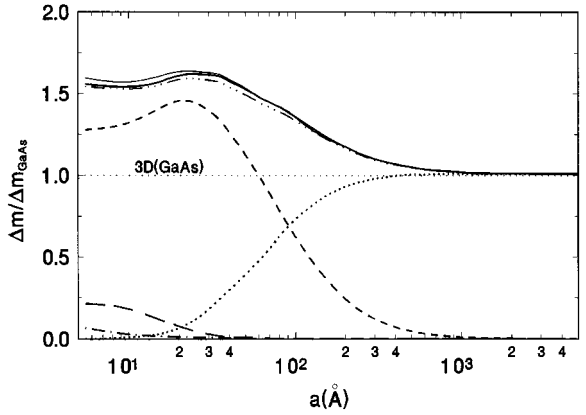

FIG. 6. Same as in Fig. 5, but for the polaron effective mass.

Figure 6 indicates the polaron effective mass for a structure corresponding to that in Fig. 5. We can see that the situation of the contributions of different phonon modes to the polaron effective mass is analogous to that of the contributions to the polaron binding energy shown in Fig. 5. The influence of the subband nonparabolicity on the polaron effective mass in step QW's is also trivial.

Moreover, we have also further calculated the polaron binding energy in asymmetric QW's $Al_{0.2}Ga_{0.8}As/GaAs/Al_{0.4}Ga_{0.6}As$ and $Al_{x_1}Ga_{1-x_1}As/GaAs/Al_{0.3}Ga_{0.7}As$ and symmetric QW's $Al_{0.3}Ga_{0.7}As/GaAs/Al_{0.3}Ga_{0.7}As$. The results are very similar to Figs. 2 and 4.

IV. SUMMARY

In this paper, we investigated the ground-state polaron binding energy and effective mass in asymmetric single and step QW's by using the second-order perturbation theory and the modified LLP variational method, in which the full energy spectrum and all possible phonon modes are all included. The effects of the finite electronic confinement potential and the subband nonparabolicity are also considered in our calculations. Comparing our results obtained by using two different methods, a good agreement is found. The main conclusions obtained in the present paper are summarized as follows.

(1) The electron extended-state wave function and the density of states in step QW's are correctly derived for the first time, to our knowledge. The extended-state wave function in QW's is a standing wave but not a propagating one.

(2) The polaron effect is closely related to the interface phonon dispersion in QW's.

(3) The contribution of the continuous spectrum to the polaron binding energy approaches approximately 80% of the total polaron binding energy at a well width $a=16$ Å and 15% in the case $a>30$ Å. Therefore, it is necessary to include the continuous energy spectrum as intermediate states in the second-order perturbation calculation for the polaron binding energy and effective mass in order to obtain the correct results.

(4) For $GaAs/Al_xGa_{1-x}As$ QW's, our results show that the contribution of half-space LO phonons to the polaron effects comes mainly from the continuous energy spectrum above the barrier and is important for narrow well width, for instance, the well width $a<100$ Å. However, the contributions of the IO modes and the confined bulklike LO modes in the well layer to the polaron effects due to the continuous energy spectrum are smaller than those of the discrete energy levels in the well. For neither too wide nor too narrow quantum wells, the polaron binding energy and effective mass come mainly from the contribution of the IO modes, and are determined by the confined bulklike LO modes in the well layer when the well width is large.

(5) The influence of the asymmetry of QW's on the polaron states is significant when the well width a is small, for instance, $a<300$ Å. However, the influence of the asymmetry can be neglected when the well width is large.

(6) The polaron binding energy and effective mass are complicated functions of the well width in QW's. When the well width and one side barrier height of asymmetric single QW's are fixed and identical with those of symmetric QW's, the polaron binding energy and effective mass in asymmetric QW's are always less than those in symmetric QW's.

(7) In $GaAs/Al_xGa_{1-x}As$ symmetric single QW's, the polaron binding energy and effective mass go continuously from the 3D $Al_xGa_{1-x}As$ to the 3D GaAs results when the well width varies from zero to infinity. This indicates that the sum of all phonon modes may look bulklike, and thus bulk-phonon approximations in QW's may remain reasonably accurate. This is in agreement with the sum rule of Refs. 44–46.

(8) For $GaAs/Al_xGa_{1-x}As$ step QW's, the influence of the well width on the polaron states is much more obvious than that of the step width.

(9) The subband nonparabolicity has a small influence on the polaron properties in QW's.

As stated above, the polaron effect has a close relation to the potential parameters of the QW's. The results obtained in this paper are very useful for further investigating the po-

laron properties and the optical and transport properties and the D^- centers in step and asymmetric single QW's and have significant meanings for analyzing experimental results, and for some important optoelectric device designs and applications in the near future.

ACKNOWLEDGMENTS

This work was supported by the National Natural Science Foundation of China and by the Natural Science Foundation of Henan Province of China.

*Mailing address.
†Present address: Institute 22, Ministry of Electronic Industry, Xinxiang 453003, Henan, P.R. China.
‡Mailing address.

[1] T. K. Mitra, A. Chatterjee, and S. Mukhopadhyay, Phys. Rep. **153**, 91 (1987).
[2] F. M. Peeters and J. T. Devreese, in *Solid State Physics*, edited by F. Seitz and D. Turnbull (Academic, New York, 1984), Vol. 38, p. 81.
[3] T. D. Lee, F. E. Low, and D. Pines, Phys. Rev. **90**, 297 (1953).
[4] L. D. Landau and S. I. Pekar, Zh. Eksp. Teor. Fiz. **16**, 341 (1946) [Sov. Phys. JETP **18**, 341 (1948)].
[5] J. J. Licari, Solid State Commun. **29**, 625 (1979).
[6] X. X. Liang, S. W. Gu, and D. L. Lin, Phys. Rev B **34**, 2807 (1986).
[7] M. H. Degani and O. Hipólito, Surf. Sci. **196**, 459 (1988).
[8] D. L. Lin, R. Chen, and T. F. George, J. Phys. Condens. Matter **3**, 4645 (1991).
[9] G. Q. Hai, F. M. Peeters, and J. T. Devreese, Phys. Rev. B **48**, 4666 (1993).
[10] Chuan-Yu Chen, Shi-Dong Liang, and Ming Li, J. Phys. Condens. Matter **6**, 1903 (1994).
[11] Shiliang Ban, X. X. Liang, and Ruisheng Zheng, Phys. Rev. B **51**, 2351 (1995).
[12] Feng-Qi Zhao, Xu Wang, and Xi-Xia Liang, Phys. Lett. A **175**, 225 (1993).
[13] R. Haupt and L. Wendler, Solid State Commun. **89**, 741 (1994).
[14] L. Wendler, A. V. Chaplik, R. Haupt, and O. Hipólito, J. Phys. Condens. Matter **5**, 8031 (1993).
[15] G. Q. Hai, F. M. Peeters, and J. T. Devreese, Phys. Rev. B **47**, 10 358 (1993).
[16] Bao-hua Wei, Xun-jie Zhao, and Shi-wei Gu, Phys. Rev. B **41**, 1368 (1990).
[17] A. Ercelebi and M. Tomak, Solid State Commun. **54**, 883 (1985).
[18] E. P. Pokatilov, S. I. Beril, V. M. Fomin, and G. Yu. Riabukhin, Phys. Status Solidi B **156**, 225 (1989).
[19] G. A. Farias, M. H. Degani, and O. Hipólito, Phys. Rev. B **43**, 4113 (1991).
[20] A. Elangovan and K. Navaneethakrishnan, J. Phys. Condens. Matter **5**, 4021 (1993).
[21] Tian-Quan Lu and Jin-Song Li, J. Phys. Condens. Matter **5**, 3365 (1993).
[22] Hai-Yang Zhou and Shi-Wei Gu, Solid State Commun. **88**, 291 (1993).
[23] A. Elangovan, D. Shyamala, and K. Navaneethakrishnan, Solid State Commun. **89**, 869 (1994).
[24] Hai-Yang Zhou and Shi-Wei Gu, Solid State Commun. **89**, 937 (1994).
[25] A. Thilagam and J. Singh, Phys. Rev. B **49**, 13 583 (1994).
[26] Ruisheng Zheng, Shiliang Ban, and Xi Xia Liang, Phys. Rev. B **49**, 1796 (1994).
[27] C. Y. Chen, D. L. Lin, P. W. Jin, S. Q. Zhang, and R. Chen, Phys. Rev. B **49**, 13 680 (1994).
[28] Bao-hua Wei, K. W. Yu, and Fa Ou, J. Phys. Condens. Matter **6**, 1893 (1994).
[29] Bao-hua Wei and K. W. Yu, J. Phys. Condens. Matter **7**, 1059 (1995).
[30] D. D. Coon and R. P. G. Karunasiri, Appl. Phys. Lett. **45**, 649 (1984).
[31] Jun-jie Shi, Ling-xi Shangguan, and Shao-hua Pan, Phys. Rev. B **47**, 13 471 (1993).
[32] Jun-jie Shi and Shao-hua Pan, Phys. Rev. B **51**, 17 681 (1995).
[33] Jun-jie Shi, Shao-hua Pan, and Zi-xin Liu, Z. Phys. B **100**, 353 (1996).
[34] Jun-jie Shi, Zi-xin Liu, and Shao-hua Pan, Superlatt. Microstruct. **17**, 329 (1995).
[35] Xi-xia Liang, J. Phys. Condens. Matter **4**, 9769 (1992).
[36] Wenhui Duan, Jia-Lin Zhu, and Bin-Lin Gu, Phys. Rev. B **49**, 14 403 (1994).
[37] D. F. Nelson, R. C. Miller, and D. A. Kleinman, Phys. Rev. B **35**, 7770 (1987).
[38] A. Messiah, *Mécanique Quantique I* (Dunod, Paris, 1973).
[39] G. Bastard, Phys. Rev. B **24**, 5693 (1981).
[40] E. N. Economou, *Green's Functions in Quantum Physics* (Springer-Verlag, Berlin, 1979).
[41] G. P. Ru and A. Z. Li, Superlattices Microstruct. **13**, 289 (1993).
[42] Kui-juan Jin, Shao-hua Pan, and Guo-zhen Yang, Phys. Rev. B **50**, 8584 (1994).
[43] S. Adachi, J. Appl. Phys. **58**, R1 (1985).
[44] K. Hess and G. Iafrate, in *Heterojunctions: Band Discontinuities and Device Applications*, edited by F. Capasso and G. Margaritondo (North-Holland, Amsterdam, 1987), pp. 451–487.
[45] N. Mori and T. Ando, Phys. Rev. B **40**, 6175 (1989).
[46] L. F. Register, Phys. Rev. B **45**, 8756 (1992).